Ion- and electron-acoustic solitons in two-electron temperature space plasmas

G. S. Lakhina,[1,a)] A. P. Kakad,[1] S. V. Singh,[1] and F. Verheest[2,3]
[1]*Indian Institute of Geomagnetism, New Panvel (West), Navi Mumbai-410 218, India*
[2]*Sterrenkundig Observatorium, Universiteit Gent, Krijgslaan 281, B-9000 Gent, Belgium*
[3]*School of Physics, University of KwaZulu-Natal, Private Bag X54001, Durban 4000, South Africa*

(Received 22 February 2008; accepted 21 April 2008; published online 9 June 2008)

Properties of ion- and electron-acoustic solitons are investigated in an unmagnetized multicomponent plasma system consisting of cold and hot electrons and hot ions using the Sagdeev pseudopotential technique. The analysis is based on fluid equations and the Poisson equation. Solitary wave solutions are found when the Mach numbers exceed some critical values. The critical Mach numbers for the ion-acoustic solitons are found to be smaller than those for electron-acoustic solitons for a given set of plasma parameters. The critical Mach numbers of ion-acoustic solitons increase with the increase of hot electron temperature and the decrease of cold electron density. On the other hand, the critical Mach numbers of electron-acoustic solitons increase with the increase of the cold electron density as well as the hot electron temperature. The ion-acoustic solitons have positive potentials for the parameters considered. However, the electron-acoustic solitons have positive or negative potentials depending whether the fractional cold electron density with respect to the ion density is greater or less than a certain critical value. Further, the amplitudes of both the ion- and electron-acoustic solitons increase with the increase of the hot electron temperature. Possible application of this model to electrostatic solitary waves observed on the auroral field lines by the Viking spacecraft is discussed. © *2008 American Institute of Physics*.
[DOI: 10.1063/1.2930469]

I. INTRODUCTION

Electrostatic solitary waves (ESWs) have been observed throughout the Earth's magnetosphere at narrow boundaries, e.g., the plasma sheet boundary layer,[1] the polar cap boundary layer,[2,3] the magnetosheath,[4] the bow shock,[5] and in strong currents, such as those associated with the auroral acceleration region.[6,7] The electrostatic solitary structures are found in the electric field parallel to the background magnetic field, and are usually bipolar or tripolar. The solitary structures found in the ion beam regions of the auroral zone[8–10] usually have negative potentials. These have been interpreted in terms of ion solitary waves or solitons.[10–14]

In the other regions mentioned above, the solitary waves are usually positive potential structures moving at velocities comparable to the electron thermal velocity (~1000s of km s^{-1}) and are commonly interpreted to be either electron holes, such as Bernstein–Greene–Kruskal (BGK) modes[15–18] arising from the evolution of a bump-on-tail instability and/or of a electron two stream instability[19,21,22] or in terms of electron-acoustic solitary waves.[20,23–28] For a detailed discussion of various models, one can refer to Lakhina *et al.*[29,30]

The earlier models based on electron-acoustic solitons could explain the space observations of solitary waves which had negative potentials in two/three temperature electron plasmas.[14,20,23–28] To explain the positive structures, attempts have been made to study electron-acoustic solitons in three-electron (cold, hot, beam) component plasmas.[31–34] These models show that depending on the beam density and temperature and below a critical velocity of the electron beam, nonlinear structures can have a positive potential signature. Berthomier *et al.*[34] have developed a 3D electron-acoustic beam model to explain the 3D shape of the solitary structures observed by FAST.[6] Recently, Verheest *et al.*[35] have pointed out the possibility to obtain compressive electron-acoustic solitons, those having positive potentials, even without the electron-beam component, provided the hot electron inertia is retained in the analysis. More recently, Kakad *et al.*[36] have studied electron-acoustic solitons in a four-component unmagnetized plasma system consisting of cold background electrons, a cold electron beam, and two types of ion species, i.e., cold and hot ions having Boltzmann distributions. This model predicts the coexistence of rarefactive and compressive electron-acoustic solitary modes for specific plasma parameters. Ghosh *et al.*[37] have studied electron-acoustic solitary waves in a four-component magnetized plasma consisting of warm electrons, warm electron beam, and two types of hot ions. They find that the ions temperature and concentration control the characteristics and the existence domain of the positive potential electron-acoustic solitons.

Observations indicate that both ion and electron beams can drive the broadband electrostatic waves.[38–41] These solitary waves have amplitudes typically a few mV/m in the plasma sheet boundary layer, but they can be as large as 200 mV/m at polar altitudes.[42] Such nonlinear solitary structures observed in the plasma sheet boundary layer and on auroral field lines may play a key role in supporting parallel electric fields in these regions.

[a)]Author to whom correspondence should be addressed. Electronic mail: lakhina@iigs.iigm.res.in.

The spacecraft observations[38–41] in the Earth's plasma sheet boundary layer show the existence of cold and hot electrons (or sometimes electron beams) having energies of the order of a few eV to a few keV, respectively, and background cold ions and warm ions and/or ion beams with energies from a few keV to tens of keV. Here, we study a three-component plasma system consisting of cold and hot electrons and hot ions. We develop a general formalism employing a multifluid approach for all the species. Thus, the restrictive assumption of treating the hot electrons and/or hot ions as having Boltzmann distributions considered in many earlier studies[14,25,37] is removed in the present analysis. Furthermore, each species can have an arbitrary beam velocity.

II. MODEL

We consider an infinite, collisionless and unmagnetized plasma consisting of three components, namely, cold electrons (N_{ce}, T_{ce}, v_{ce}), hot electrons (N_{he}, T_{he}, v_{he}), and ions (N_i, T_i, v_i), where N_j, T_j, v_j represents the density, temperature and beam velocity (along the direction of wave propagation) of the species j, and $j=ce$, he, and i for the cold electrons, hot electrons, and the ions, respectively. We treat all the species as mobile. Then, their dynamics are governed by the multifluid equations of continuity, momentum and equation of state of each species, and the Poisson equation,

$$\frac{\partial n_j}{\partial t}+\frac{\partial (n_j v_j)}{\partial x}=0, \tag{1}$$

$$\frac{\partial v_j}{\partial t}+v_j\frac{\partial v_j}{\partial x}+\frac{1}{\mu_j n_j}\frac{\partial P_j}{\partial x}-\frac{Z_j}{\mu_j}\frac{\partial \phi}{\partial x}=0, \tag{2}$$

$$\frac{\partial P_j}{\partial t}+v_j\frac{\partial P_j}{\partial x}+3P_j\frac{\partial v_j}{\partial x}=0, \tag{3}$$

$$\frac{\partial^2 \phi}{\partial x^2}=n_{ce}+n_{he}-n_i. \tag{4}$$

Further, all densities are normalized with the unperturbed ion density, $N_i=N_{ce}+N_{he}$, velocities with the ion thermal velocity $C_i=(T_i/m_i)^{1/2}$ (here, m_j represents the mass of the jth species), time with the ion plasma frequency, $\omega_{pi}=(4\pi N_i e^2/m_i)^{1/2}$, the lengths with the ion Debye length, $\lambda_{di}=(T_i/4\pi N_i e^2)^{1/2}$, and the thermal pressures P_j with $N_i T_i$. Furthermore, we have assumed the same adiabatic index, i.e., $\gamma=3$, for all the species in the equation of state given by Eq. (3).

To study the properties of stationary arbitrary amplitude ESWs, we transform the above set of equations to a stationary frame moving with velocity V, the phase velocity of the wave, i.e., $\xi=x-Mt$, where $M=V/C_i$ is the Mach number with respect to the ion thermal velocity. Then, solving for perturbed densities, putting these expressions in the Poisson equation, and assuming appropriate boundary conditions for the localized disturbances along with the conditions that $\phi=0$, and $d\phi/d\xi=0$ at $\xi\rightarrow\pm,\infty$, we get the following energy integral:

$$\frac{1}{2}\left(\frac{\partial \phi}{\partial \xi}\right)+\psi(\phi,M)=0, \tag{5}$$

where

$$\psi(\phi,M)=\mu_{ei}n_{ce}^0\left[(M-v_{ce})^2-\frac{(M-v_{ce})}{\sqrt{2}}B_{ce}^{1/2}\right]+n_{ce}^0T_{ce}[1-2\sqrt{2}(M-v_{ce})^3B_{ce}^{-3/2}]+\mu_{ei}n_{he}^0\left[(M-v_{he})^2-\frac{(M-v_{he})}{\sqrt{2}}B_{he}^{1/2}\right]$$
$$+n_{he}^0T_{he}[1-2\sqrt{2}(M-v_{he})^3B_{he}^{-3/2}]+n_i^0\left[(M-v_i)^2-\frac{(M-v_i)}{\sqrt{2}}B_i^{1/2}\right]+n_i^0[1-2\sqrt{2}(M-v_i)^3B_i^{-3/2}] \tag{6}$$

is the pseudopotential, also known as the Sagdeev potential. Here,

$$B_{ce}=A_{ce}+\sqrt{A_{ce}^2-\frac{12T_{ce}(M-v_{ce})^2}{\mu_{ei}}},$$

$$B_{he}=A_{he}+\sqrt{A_{he}^2-\frac{12T_{he}(M-v_{he})^2}{\mu_{ei}}},$$

$$B_i=A_i+\sqrt{A_i^2-12(M-v_i)^2},$$

$$A_{ce}=(M-v_{ce})^2+\frac{3T_{ce}}{\mu_{ei}}+\frac{2\phi}{\mu_{ei}},$$

$$A_{he}=(M-v_{he})^2+\frac{3T_{he}}{\mu_{ei}}+\frac{2\phi}{\mu_{ei}},$$

$$A_i=(M-v_i)^2+3-2\phi,\quad \mu_{ei}=\frac{m_e}{m_i}.$$

Further, in Eq. (6), $n_j^0=N_j/N_i$ such that $n_{ce}^0+n_{he}^0=n_i^0=1$, and the temperatures of the species are normalized with the ion temperature.

III. NONLINEAR ELECTROSTATIC SOLITARY WAVES (ESWS)

Equation (5) yields solitary wave solutions when the Sagdeev potential $\psi(\phi,M)$ satisfies the following conditions: $\psi(\phi,M)=0$, $d\psi(\phi,M)/d\phi=0$, $d^2\psi(\phi,M)/d\phi^2<0$ at $\phi=0$;

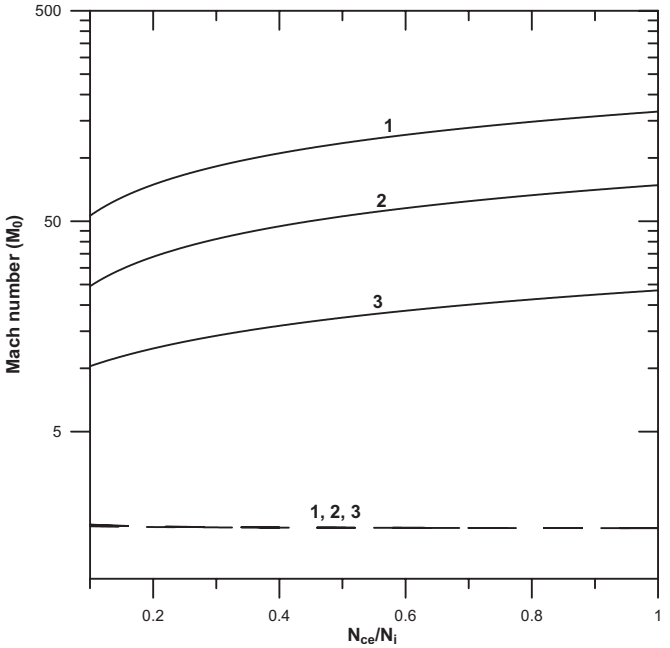

FIG. 1. Plot of critical Mach numbers obtained from Eq. (7) vs cold electron to ion number density ratio for the parameters, $T_{ce}/T_i=0.01$ and $T_{he}/T_i=5.0$, 1.0, and 0.1 for the curves 1, 2, and 3, respectively. Here, flow velocity of all species is taken as 0. The dashed curves are for the ion-acoustic modes, whereas the solid curves are for the electron-acoustic modes. The soliton solutions exist only in a small region above each curve.

$\psi(\phi,M)=0$ at $\phi=\phi_0$, and $\psi(\phi,M)<0$ for $0<|\phi|<|\phi_0|$. From Eq. (6) it is seen that $\psi(\phi,M)$ and its first derivative with respect to ϕ vanish at $\phi=0$. The condition $d^2\psi(\phi,M)/d\phi^2<0$ at $\phi=0$ is satisfied provided $M>M_0$, where M_0 satisfies the equation

$$f(M_0)\equiv \frac{n_{ce}^0}{\mu_{ei}\left[(M_0-v_{ce})^2-\frac{3T_{ce}}{\mu_{ei}}\right]} + \frac{n_{he}^0}{\mu_{ei}\left[(M_0-v_{he})^2-\frac{3T_{he}}{\mu_{ei}}\right]} + \frac{n_i^0}{[(M_0-v_{hi})^2-3]} = 0. \quad (7)$$

Equation (7) yields 4 roots but all the roots will not be physical. We will consider here only the real positive roots for M_0, or the critical Mach numbers. Numerical solution of Eq. (7) for $T_{ce}\ll T_i$ shows the existence of two critical Mach numbers which satisfy all the soliton conditions. Figure 1 shows the roots of Eq. (7) for different values of T_{he}/T_i and the ratio of cold electron to ion number density, N_{ce}/N_i. The lower roots (shown as dashed curves) are most likely the ion-acoustic modes, whereas the higher roots (shown as solid curves) are the electron-acoustic modes (see Ref. 43). Further, in a fluid dynamic formalism, when inertia for all species is retained (as done here), the respective Mach numbers are limited by sonic points, where the flow of one species is choked.[44,45] The critical Mach numbers correspond to this situation.

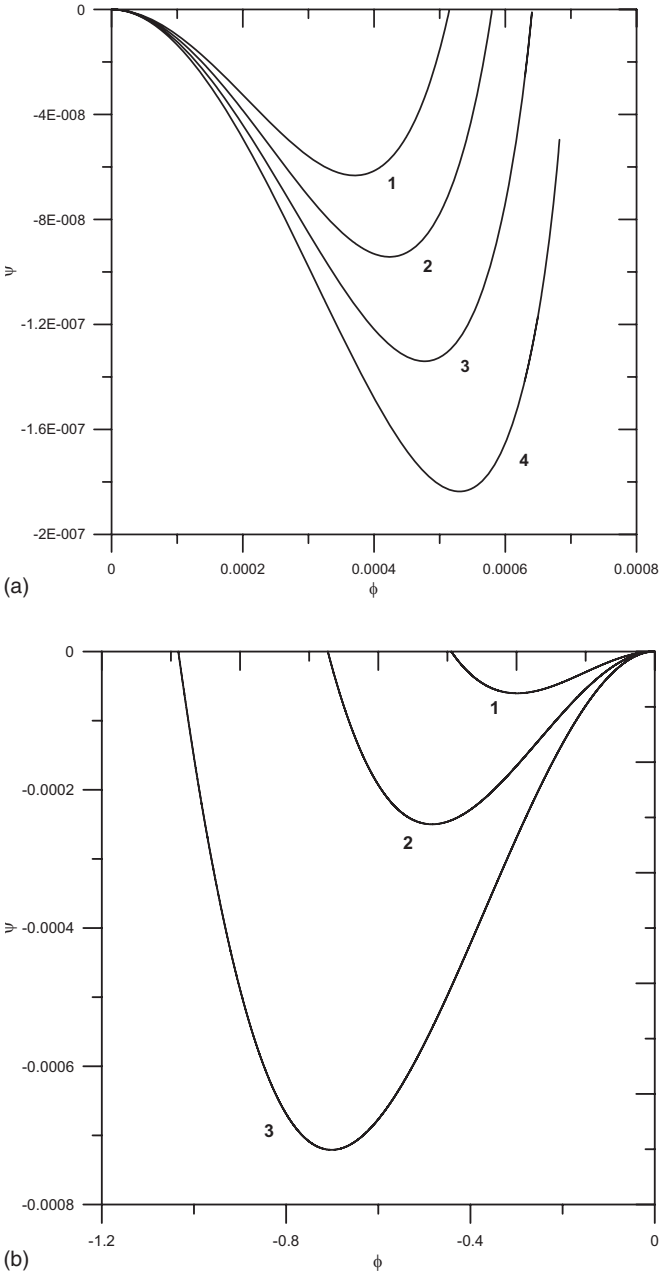

FIG. 2. (a) Ion-acoustic solitons for plasma parameters, $N_{ce}/N_i=0.3$, $T_{ce}/T_i=0.01$, and $T_{he}/T_i=5.0$, and for the Mach number $M=1.766$, 1.767, 1.768, 1.769 for the curves 1, 2, 3, and 4, respectively. (b) Electron-acoustic solitons for the same plasma parameters as in Fig. 2(a), but for the Mach number $M=93.0$, 94.0, and 95.0 for the curves 1, 2, and 3, respectively.

From Fig. 1, it is seen that the critical Mach numbers for the electron-acoustic modes increase with the increase in density ratio N_{ce}/N_i as well as the temperature ratio T_{he}/T_i (see solid curves 1, 2, and 3). The critical Mach number for the ion acoustic modes show a slight reduction when N_{ce}/N_i increases or T_{he}/T_i decreases. The changes are so small that these are not discernible (see dashed curves 1, 2, and 3) on the scale used in Fig. 1.

We have numerically solved Eq. (6) for the Sagdeev potential, $\psi(\phi,M)$, as a function of ϕ for various values of Mach numbers and for some typical plasma parameters. The results are shown in Figs. 2(a) and 2(b) and Figs. 3(a) and

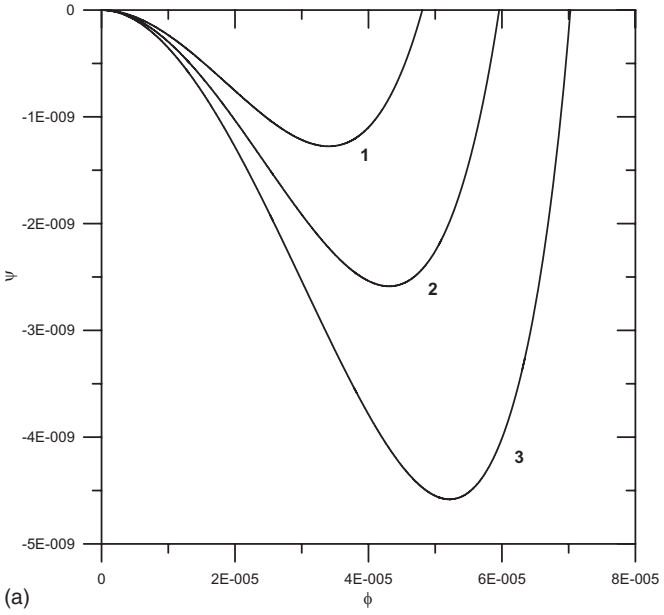

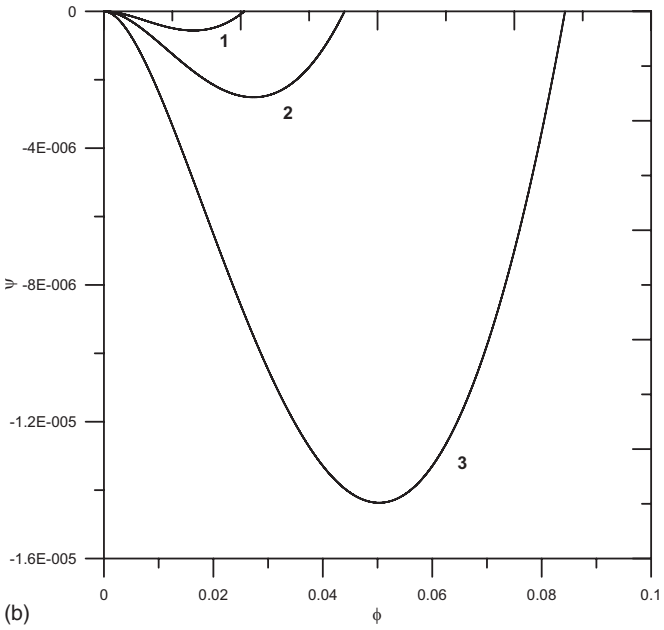

FIG. 3. (a) Ion-acoustic solitons for the same plasma parameters as in Fig. 2(a) except that $N_{ce}/N_i=0.9$. The Mach number $M=1.7430$, 1.7435, 1.7440 for the curves 1, 2, and 3, respectively. (b) Electron-acoustic solitons for the same plasma parameters as in Fig. 3(a), and for the Mach number $M=159.0$, 160.0, and 162.0 for the curves 1, 2, and 3, respectively.

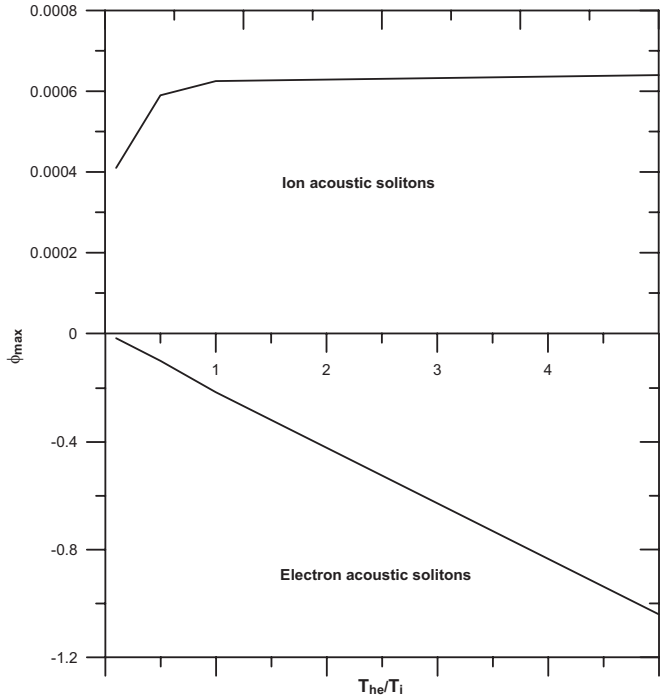

FIG. 4. Variation of $\phi_{\max}$, the maximum value of ϕ_0 corresponding to $M_{\max}$ (beyond which solitary solutions do not exist) vs hot electron to ion temperature ratio, T_{he}/T_i for the case of $N_{ce}/N_i=0.3$, $T_{ce}/T_i=0.01$.

3(b). Here, we have omitted all beam velocities. The solitary wave solutions of both ion- and electron-acoustic modes are found when the Mach numbers exceed the critical values (e.g., as found in Fig. 1).

In Fig. 2(a) it is seen that the ion-acoustic solitons have positive potentials. The maximum electrostatic potential ϕ_0 increases with the increase of the Mach number, M, as seen from curves 1, 2, and 3 of Fig. 2(a). For curve 4, the soliton solution does not exist. Hence there is an upper value for M, say $M_{\max}$, above which soliton solutions do not exist. This is true for ion-acoustic as well as for electron-acoustic solitary structures. Figure 2(b) shows that for the same plasma parameters, but for higher values of the Mach number, M, electron-acoustic solitons can exist. However, the electron-acoustic solitons have negative potentials. In this case also the maximum electrostatic potential ϕ_0 increases with an increase in M.

Figures 3(a) and 3(b) show the variation of $\psi(\phi,M)$ versus ϕ for the same plasma parameters as in Figs. 2(a) and 2(b) except for N_{ce}/N_i. Here $N_{ce}/N_i=0.9$, whereas it is 0.3 in Figs. 2(a) and 2(b). Here, both the ion-acoustic [Fig. 3(a)] and the electron-acoustic [Fig. 3(b)] solitons have positive potentials. For both types of solitons, ϕ_0 increases with M.

For the parameters considered for the computations, the model supports only positive potential ion acoustic solitons. However, it can support positive or negative potential electron-acoustic solitons depending on the fractional cold electron density, i.e., the ratio $R=N_{ce}/N_i$. Starting from small values of R, a change over from negative to positive potential structures occurs when R exceed a certain critical value, which depends on the plasma parameters. For example, for the case of $T_{ce}/T_i=0.01$, $T_{he}/T_i=1.0$ and no beams, the electron-acoustic solitons have negative potentials for $R<0.43$ and positive potentials when $R\geqslant 0.43$.

In Fig. 4, we have shown $\phi_{\max}$, the maximum value of ϕ_0 corresponding to $M_{\max}$ (beyond which solitary solutions do not exist), for different values of the hot electron to ion temperature ratio, T_{he}/T_i.

From Fig. 4, it is seen that the ion-acoustic solitons have positive potentials which first increases with T_{he}/T_i and then saturates. The electron-acoustic solitons have negative potential, and the magnitude of $\phi_{\max}$ increases monotonically with an increase of T_{he}/T_i. Similar behavior is also seen at other densities. However, at higher cold electron densities, i.e.,

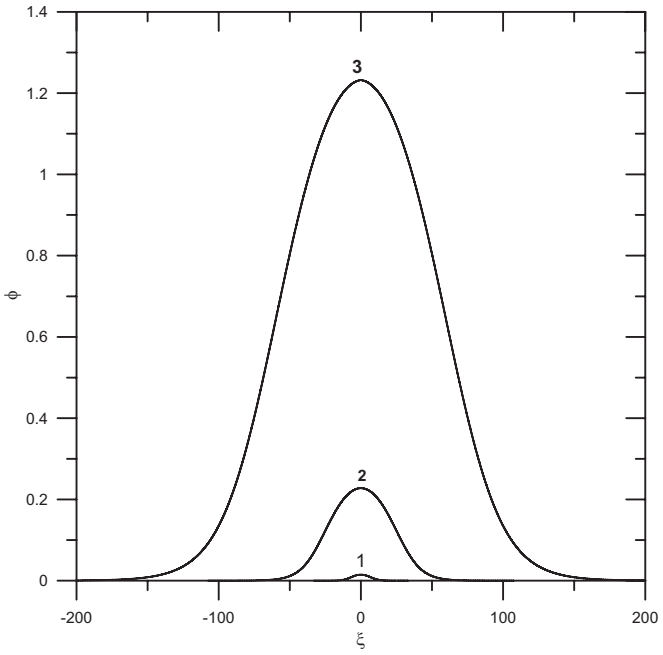

FIG. 5. Shows variation of the electron-acoustic potential ϕ vs ξ for $N_{ce}/N_i=0.5$, $T_{ce}/T_i=0.01$, and for $T_{he}/T_i=0.1$, 1.0, and 5.0 for the curves 1, 2, and 3, respectively. The Mach number $M=17.55$, 53.40, and 119.0 for the curves 1, 2, and 3, respectively.

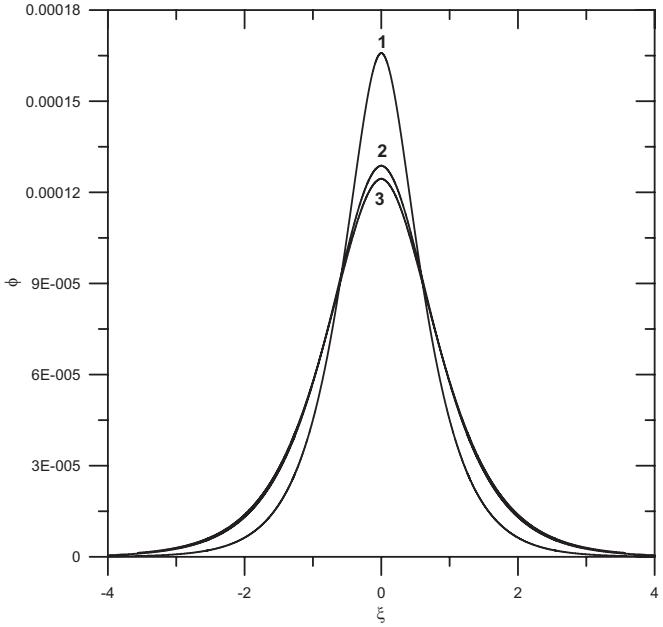

FIG. 6. Shows the variation of the ion-acoustic potential ϕ vs ξ for $N_{ce}/N_i=0.5$, $T_{ce}/T_i=0.01$, and for $T_{he}/T_i=0.1$, 1.0, and 5.0 for the curves 1, 2, and 3, respectively. Here, the Mach number $M=1.751$ for all the curves.

$N_{ce}/N_i \geqslant 0.5$, the electron-acoustic solitons have positive potentials, and the $\phi_{\max}$ magnitude once again increases monotonically with T_{he}/T_i.

In Fig. 5, we have shown the profiles for the potential, ϕ, of the electron-acoustic solitons for different values of the hot electron to ion temperature ratio, T_{he}/T_i, for the case of $N_{ce}/N_i=0.5$, $T_{ce}/T_i=0.01$. It is seen that both the amplitude and the width of the electron-acoustic solitons increase with the increase of T_{he}/T_i (cf. curves 1, 2, and 3). From the curves 1, 2, and 3, it seen that the maximum value of the potential, $\phi_{\max}=0.014$, 0.23, and 1.2, and the associated soliton width, W, defined as full width at half maximum is $W=12.5$, 50, and 125 for $T_{he}/T_i=0.1$, 1.0, and 5.0, respectively. The electric field associated with the solitary potential profile will have a bipolar structure as can be verified by differentiating the profiles.

In Fig. 6, we have shown the profiles for the potential, ϕ, of the ion-acoustic solitons for the same plasma parameters as in Fig. 5. In this case, the maximum soliton amplitudes decrease with the increase of T_{he}/T_i (cf. curves 1, 2, and 3), though slightly. The maximum potential $\phi_{\max}$ varies from 0.00012 to 0.00016 when T_{he}/T_i is increased from 0.1 to 5.0. Similarly, the variation of T_{he}/T_i does not affect the soliton width significantly, though W has a slight increase initially from 1.44 to 1.5, and then decreases to 1.25 as T_{he}/T_i varies from 0.1 to 5.0.

IV. DISCUSSION

We have described a general analysis for studying large-amplitude ion- and electron-acoustic solitary waves in an unmagnetized plasma consisting of two, cold and hot, electron populations and one type of ion population. The model treats all the species as mobile, and in principle all species can have an arbitrary beam velocity. For simplicity, we have presented numerical results for the cases where the beams are absent. The effects of the beams on the critical Mach numbers and soliton characteristics will be discussed elsewhere.

We would like to point out that we have assumed the same adiabatic equation of state with $\gamma=3$ for all species. It allows an analytical expression of the Sagdeev pseudopotential, and has the advantage of keeping for all species both inertial and thermal terms in their dynamics. Comparison with the Berthomier *et al.*[31,34] papers shows that they need beams or more electron species to get positive potentials electron-acoustic solitons. Further, since we deal with the one-dimensional problem in an unmagnetized plasma system, choosing $\gamma=3$ appears to be appropriate as particles have essentially one degree of freedom along the wave propagation direction. On the other hand, Berthomier *et al.*[34] deal with a magnetized plasma case, in which particle motions parallel and perpendicular to the magnetic field are quite different. In such a case, the choice of different γ*s* along parallel and perpendicular directions with respect to the magnetic field appears to be necessary and justified.

The most important results of the present model is that the electron-acoustic ESWs can have either negative or positive potential depending on R, the fractional number density of the cold electrons relative to that of the ions (or total electrons). For R exceeding a critical value, positive potential electron-acoustic ESWs can exist. However, the ion acoustic solitons are found to have positive potentials for all values of R for the parameter considered here.

From Figs. 5 and 6, we note that for T_{he}/T_i varying from 0.1 to 5.0, the typical widths of the ion- and electron-acoustic solitons are $W \sim (1.25-1.5)$ and (12.5–125), respectively.

The maximum normalized potentials, $\phi_{\max}$, for the ion- and electron-acoustic solitons are found to be $\sim(0.00012-0.00016)$ and (0.014–1.2), respectively. It is interesting to note that the electric fields associated with the ion- and electron-acoustic solitons would have bipolar structures with maximum amplitudes, $E_{\max}\approx(T_i\phi_{\max}/e\lambda_{di}W)$. For the case of $R=0.5$, $T_{ce}=1$ eV, $T_i=100$ eV, and $T_{he}=(10-500)$ eV and $N_i=3$ cm^{-3}, we have $\lambda_{di}\approx 43$ m, and the maximum electric field comes out to be $E_{\max}\sim(0.2-0.3)$ mV/m for the ion-acoustic solitons and (2–22) mV/m for the electron-acoustic solitons.

As mentioned in the Introduction, several attempts have been made to explain the positive potential ESWs observed in different regions of the magnetosphere in terms of electron-acoustic solitons in three-electron (cold, hot, beam) component plasmas.[32–34] The presence of the electron beam was an essential ingredient of these models. Our model shows that the presence of the electron beam is not necessary for the existence of positive potential electron-acoustic solitons, rather it is the inertia of the species which plays the crucial role.

The analysis presented here is general and can be applied to many space observations of electrostatic solitary structures where two types of electron populations, namely, cold and hot, and ions are observed, such as in the cusp and the auroral field lines. The Viking satellite frequently observed cold and hot electrons at the times of bursts of ESWs in the auroral region.[24] Typical parameter associated with the burst *b* (refer to Table 2 of Dubouloz *et al.*[24]) are: Cold electron density of 0.2 cm^{-3}, hot electron density of $\sim$1.5 cm^{-3}, and beam electron density of 1.0 cm^{-3}; cold electron temperature $T_{ce}=2$ eV, and electron beam temperature
$T_b=50$ eV, hot electron temperature $T_{he}=250$ eV. Treating the cold electron and the beam as a single species with density $N_{ce}=1.2$ cm^{-3}, we get $R=N_{ce}/N_i=1.2/2.7=0.444$, $T_{ce}/T_i=0.01$, and $T_{he}/T_i=1.25$, if we take $T_i=200$ eV. These normalized parameters are very close to that of the curve 2 in Figs. 5 and 6. Therefore, we expect both ion- and electron-acoustic solitons to have positive potentials. The electric fields will be bipolar with maximum amplitudes of the order of 0.2 mV/m for the ion-acoustic solitons and $\sim$10 mV/m for the electron-acoustic solitons. The width of these ESWs would be $\sim$60 m and 2.0 km, respectively. These estimates compare favorably with the Viking observations.

ACKNOWLEDGMENTS

G.S.L. thanks the Council of Scientific and Industrial Research, Government of India, for the support under the Emeritus Scientist scheme. F.V. thanks the Indian Institute of Geomagnetism for its kind hospitality when the paper was finalized and also the Fonds voor Wetenschappelijk Onderzock (Vlaanderen) for a research grant.

[1] H. Matsumoto, H. Kojima, T. Miyatake, Y. Omura, M. Okada, I. Nagano, and M. Tsutui, Geophys. Res. Lett. **21**, 2915, DOI: 10.1029/94GL01284 (1994).
[2] J. R. Franz, P. M. Kintner, and J. S. Pickett, Geophys. Res. Lett. **25**, 1277, DOI: 10.1029/98GL50870 (1998).
[3] B. T. Tsurutani, J. K. Arballo, G. S. Lakhina, C. M. Ho, B. Buti, J. S. Pickett, and D. A. Gurnett, Geophys. Res. Lett. **25**, 4117, DOI: 10.1029/1998GL900114 (1998).
[4] J. S. Pickett, J. D. Menietti, D. A. Gurnett, B. Tsurutani, P. Kintner, E. Klatt, and A. Balogh, Nonlinear Processes Geophys. **10**, 3 (2003).
[5] S. D. Bale, P. J. Kellogg, D. E. Larson, R. P. Lin, K. Goetz, and R. P. Lepping, Geophys. Res. Lett. **25**, 2929, DOI: 10.1029/98GL02111 (1998).
[6] R. E. Ergun, C. W. Carlson, J. P. McFadden, F. S. Mozer, G. T. Delory, W. Peria, C. C. Chaston, M. Temerin, I. Roth, L. Muschietti, R. Elphic, R. Strangeway, R. Pfaff, C. A. Cattell, D. Klumpar, E. Shelley, W. Peterson, E. Moebius, and L. Kistler, Geophys. Res. Lett. **25**, 2041, DOI: 10.1029/98GL00636 (1998).
[7] S. R. Bounds, R. F. Pfaff, S. F. Knowlton, F. S. Mozer, M. A. Temerin, and C. A. Kletzing, J. Geophys. Res. **104**, 28709, DOI: 10.1029/1999JA900284 (1999).
[8] M. Temerin, K. Cerny, W. Lotko, and F. S. Mozer, Phys. Rev. Lett. **48**, 1175 (1982).
[9] R. Boström, G. Gustafsson, B. Holback, G. Holmgren, H. Koskinen, and P. Kintner, Phys. Rev. Lett. **61**, 82 (1988).
[10] H. E. J. Koskinen, R. Lundin, and B. Holback, J. Geophys. Res. **95**, 5921, DOI: 10.1029/JA095iA05p05921 (1990).
[11] M. K. Hudson, W. Lotko, I. Roth, and E. Witt, J. Geophys. Res. **88**, 916 (1983).
[12] R. V. Reddy and G. S. Lakhina, Planet. Space Sci. **39**, 1343 (1991).
[13] R. V. Reddy, G. S. Lakhina, and F. Verheest, Planet. Space Sci. **40**, 1055 (1992).
[14] M. Berthomier, R. Pottelette, and M. Malingre, J. Geophys. Res. **103**, 4261, DOI: 10.1029/97JA00338 (1998).
[15] I. B. Bernstein, J. M. Greene, and M. D. Kruskal, Phys. Rev. **108**, 546 (1957).
[16] L. Muschietti, R. E. Ergun, I. Roth, and C. W. Carlson, Geophys. Res. Lett. **26**, 1093, DOI: 10.1029/1999GL900207 (1999).
[17] L. J. Chen, J. Pickett, P. Kinter, J. Franz, and D. Gurnett, J. Geophys. Res. **110**, A09211, DOI: 10.1029/2005JA011087 (2005).
[18] D. Jovanovic and P. K. Shukla, Phys. Rev. Lett. **84**, 4373 (2000).
[19] Y. Omura, H. Matsumoto, T. Miyake, and H. Kojima, J. Geophys. Res. **101**, 2685, DOI: 10.1029/95JA03145 (1996).
[20] H. Kojima, H. Matsumoto, S. Chikuba, S. Horiyama, M. Ashour-Abdalla, and R. R. Anderson, J. Geophys. Res. **102**, 14439, DOI: 10.1029/97JA00684 (1997).
[21] M. V. Goldman, M. M. Oppenheim, and D. L. Newman, Geophys. Res. Lett. **26**, 1821, DOI: 10.1029/1999GL900435 (1999).
[22] R. Pottelette, M. Malingre, N. Dubouloz, B. Aparicio, R. Lundin, G. Holmgren, and G. Marklund, J. Geophys. Res. **95**, 5957, DOI: 10.1029/JA095iA05p05957 (1990).
[23] N. Dubouloz, R. Pottelette, M. Malingre, and R. A. Treumann, Geophys. Res. Lett. **18**, 155 (1991).
[24] N. Dubouloz, R. A. Treumann, R. Pottelette, and M. Malingre, J. Geophys. Res. **98**, 17415, DOI: 10.1029/93JA01611 (1993).
[25] S. V. Singh, R. V. Reddy, and G. S. Lakhina, Adv. Space Res. **28**, 111643 (2001).
[26] S. V. Singh and G. S. Lakhina, Planet. Space Sci. **49**, 107 (2001).
[27] S. V. Singh and G. S. Lakhina, Nonlinear Processes Geophys. **11**, 275 (2004).
[28] S. G. Tagare, S. V. Singh, R. V. Reddy, and G. S. Lakhina, Nonlinear Processes Geophys. **11**, 215 (2004).
[29] G. S. Lakhina, B. T. Tsurutani, H. Kojima, and H. Matsumoto, J. Geophys. Res. **105**, 27791 (2000).
[30] G. S. Lakhina, B. T. Tsurutani, and J. S. Pickett, Nonlinear Processes Geophys. **11**, 11205 (2004).
[31] M. Berthomier, R. Pottelette, M. Malingre, and Y. Khotyaintsev, Phys. Plasmas **7**, 2987 (2000).
[32] R. L. Mace and M. A. Hellberg, Phys. Plasmas **8**, 2649 (2001).
[33] W. F. El-Taibany, J. Geophys. Res. **110**, A01213, DOI: 10.1029/2004JA010525 (2005).
[34] M. Berthomier, R. Pottelette, L. Muschietti, I. Roth, and C. W. Carlson, Geophys. Res. Lett. **30**, 2148, DOI: 10.1029/2003GL018491 (2003).
[35] F. Verheest, T. Cattaert, and M. Hellberg, Space Sci. Rev. **121**, 299 (2005).
[36] A. P. Kakad, S. V. Singh, R. V. Reddy, G. S. Lakhina, S. G. Tagare, and F. Verheest, Phys. Plasmas **14**, 052305 (2007).
[37] S. Ghosh, J. S. Pickett, G. S. Lakhina, J. D. Winningham, B. Lavraud, and

P. Decreau, "Parametric analysis of positive amplitude electron acoustic solitary waves in a magnetized plasma and its application to boundary layers," J. Geophys. Res. (in press).
[38]G. K. Parks, M. McCarthy, R. J. Fitzenreiter, J. Etcheto, K. A. Anderson, R. R. Anderson, T. E. Eastman, L. A. Frank, D. A. Gurnett, C. Huang, R. P. Lin, A. T. Y. Lui, K. W. Ogilvie, A. Pederson, H. Reme, and D. J. Williams, J. Geophys. Res. **89**, 8885, DOI: 10.1029/JA089iA10p08885 (1984).
[39]G. Parks, L. J. Chen, M. McCarthy, D. Larson, R. P. Lin, T. Phan, H. Reme, and T. Sanderson, Geophys. Res. Lett. **25**, 3285, DOI: 10.1029/98GL02208 (1998).
[40]T. G. Onsager, M. F. Thomsen, R. C. Elphic, J. T. Gosling, R. R. Anderson, and G. Kettmann, J. Geophys. Res. **98**, 15509, DOI: 10.1029/93JA00921 (1993).
[41]K. Takahashi and E. W. Hones, Jr., J. Geophys. Res. **93**, 8558, DOI: 10.1029/JA093iA08p08558 (1988).
[42]C. A. Cattell, J. Dombeck, J. R. Wygant, M. K. Hudson, F. S. Mozer, M. A. Temerin, W. K. Peterson, C. A. Kletzing, C. T. Russell, and R. F. Pfaff, Geophys. Res. Lett. **26**, 425, DOI: 10.1029/1998GL900304 (1999).
[43]F. Verheest, M. A. Hellberg, and G. S. Lakhina, Astrophys. Space Sci. **3**, 15 (2007).
[44]J. F. McKenzie, E. Dubinin, K. Sauer, and T. B. Doyle, J. Plasma Phys. **70**, 431 (2004).
[45]F. Verheest, T. Cattaert, G. S. Lakhina, and S. V. Singh, J. Plasma Phys. **70**, 237 (2004).